Biomaterials 34 (2013) 2024–2037

Contents lists available at SciVerse ScienceDirect

Biomaterials

journal homepage: www.elsevier.com/locate/biomaterials

Engineered scaffold-free tendon tissue produced by tendon-derived stem cells☆

Ming Ni [a,b,1], Yun Feng Rui [a,c,1], Qi Tan [a], Yang Liu [a], Liang Liang Xu [a], Kai Ming Chan [a,d,e,***], Yan Wang [b,**], Gang Li [a,d,e,*]

[a] Department of Orthopaedics and Traumatology, Faculty of Medicine, The Chinese University of Hong Kong, Hong Kong SAR, China
[b] Department of Orthopaedics, The General Hospital of Chinese People's Liberation Army, Beijing 100853, China
[c] Department of Orthopaedics, Zhongda Hospital, School of Medicine, Southeast University, 87 Ding Jia Qiao, Nanjing, Jiangsu 210009, China
[d] The Hong Kong Jockey Club Sports Medicine and Health Sciences Centre, Faculty of Medicine, The Chinese University of Hong Kong, Hong Kong SAR, China
[e] Program of Stem Cell and Regeneration, School of Biomedical Science, and Li Ka Shing Institute of Health Sciences, Faculty of Medicine, The Chinese University of Hong Kong, Hong Kong SAR, China

ARTICLE INFO

Article history:
Received 14 September 2012
Accepted 26 November 2012
Available online 14 December 2012

Keywords:
Tendon-derived stem cells
Connective tissue growth factor
Tenogenic differentiation
Scaffold-free
Cell sheet
Tendon tissue engineering

ABSTRACT

Most of the exogenous biomaterials for tendon repair have limitations including lower capacity for inducing cell proliferation and differentiation, poorer biocompatibility and remodeling potentials. To avoid these shortcomings, we intend to construct an engineered tendon by stem cells and growth factors without exogenous scaffolds. In this study, we produced an engineered scaffold-free tendon tissue (ESFTT) in vitro and investigated its potentials for neo-tendon formation and promoting tendon healing in vivo. The ESFTT, produced via tendon-derived stem cells (TDSCs) by treatment of connective tissue growth factor (CTGF) and ascorbic acid in vitro, was characterized by histology, qRT-PCR and immunohistochemistry methods. After ESFTT implanted into the nude mouse, the in vivo fluorescence imaging, histology and immunohistochemistry examinations showed neo-tendon formation. In a rat patellar tendon window injury model, the histology, immunohistochemistry and biomechanical testing data indicated ESFTT could significantly promote tendon healing. In conclusion, this is a proof-of-concept study demonstrating that ESFTT could be a potentially new approach for tendon repair and regeneration.

1. Introduction

Tendon injuries are common in both the workplace and sport activities with more than 30 million injuries occurred annually worldwide [1]. There were about 200,000 tendon and ligament repair surgeries performed annually in the USA [2]. The reported incidence of acute Achilles tendon injury was 18 per 100,000 people [3]; and these injuries typically occurred between the ages of 20 and 50 years [4]. Rotator cuff injuries are among the most common traumatic tears, with over 50,000 rotator cuff repair surgeries performed each year in the USA [5]. These injuries are difficult to manage because tendons do not heal by a regenerative process but via formation of a fibrotic scar, with poor tissue quality and mechanical properties and frequently result in long-term pain, discomfort and disability [6]. Tendon healing occurs in three overlapping phases. In the initial inflammatory phase, inflammatory cells enter the site of injury, chemotactic factors and inflammatory cytokines are released with increased vascular permeability, initiation of angiogenesis, stimulation of tenocyte proliferation. In the repair phase, tenocytes gradually migrate to the wound, and type III collagen synthesis is initiated and peaks during this phase, which lasts for a few weeks. After approximately 4–6 weeks, the modeling phase commences, the healing tissue is reshaped with decrease in cellularity and the type III collagens are being replaced by type I collagen and other tendon related ECM proteins during the remodeling phase. The inability of tendons to self-repair and the general inefficiencies of current treatments have spurred a demand for the development of tissue-engineering strategies for tendon repair and regeneration [7].

Most of the exogenous biomaterials for tendon repair have limitations including lower capacity for inducing cell proliferation and differentiation, poorer biocompatibility and remodeling potentials. Many challenges exist in tendon tissue engineering,

☆ This study has been accepted as podium presentation in the ORS 2012 Annual Meeting in San Francisco, California, and also was the winner of "Webster Jee Young Investigator Award" at 2012 ORS-ICHTS membership meeting from the International Chinese Hard Tissue Society.

* Corresponding author. Department of Orthopaedics and Traumatology, Faculty of Medicine, The Chinese University Hong Kong, Prince of Wales Hospital, Shatin, Hong Kong, PR China. Tel.: +852 3763 6153; fax: +852 2646 3020.
** Corresponding author. Tel.: +86 10 6693 9439; fax: +86 10 8821 9862.
*** Corresponding author. Department of Orthopaedics and Traumatology, Faculty of Medicine, The Chinese University Hong Kong, Prince of Wales Hospital, Shatin, Hong Kong, PR China. Tel.: +852 2636 2728; fax: +852 2646 3020.
E-mail addresses: kmchan@cuhk.edu.hk (K.M. Chan), yanwang301@yahoo.com (Y. Wang), gangli@cuhk.edu.hk (G. Li).
[1] Ni M and Rui YF are co-first authors with equal contribution in this work.

0142-9612/$ – see front matter © 2012 Elsevier Ltd. All rights reserved.
http://dx.doi.org/10.1016/j.biomaterials.2012.11.046

such as low cell proliferation and differentiation efficiency within exogenous biomaterials, unmatched rates between exogenous scaffold degradation and cell proliferation as well as extracellular matrix production, and different biomechanical properties compared with intact tendon. With the development of cell sheet-based bioengineering concepts, cell sheet engineering can provide natural cellular junctions, extracellular matrix and microenvironments [8–12]. The current investigation intends to construct an engineered tendon by stem cells and growth factors without exogenous scaffolds.

Tendon stem/progenitor cells, as a new cell type, was firstly identified in both human and mouse tendon tissues in 2007 [13], and we also isolated and characterized this unique stem cell population from rat tendon tissues [14,15]. We have found that tendon-derived stem cells (TDSCs) have higher mRNA expression of tenomodulin (Tnmd), scleraxis (Scx), type I collagen (Col1A1), decorin (Dcn) and biglycan (Bgn) than that of bone marrow derived mesenchymal stem cells (BMSCs) [16]. Our recent study further demonstrated TDSCs could promote earlier and better recovery after tendon injury as a new cell source for tendon repair [17]. However, higher mRNA expression of osteogenic markers such as alkaline phosphatase (ALP) and osteocalcin and chondrogenic markers aggrecan (Acan) and type II collagen (Col2A1) was also detected in the TDSCs comparing with that of BMSCs in vitro [16], indicating that TDSCs may also have higher osteo-chondrogenic potentials. The ectopic bone formation in tendon after transplantation of MSCs is an unwanted side effect that had been reported [18,19]. To avoid this potential risk, we propose that tenogenic differentiation of TDSCs in vitro may promote tendon healing and alleviate the risk of complication such as ectopic bone formation after transplantation of tenogenic TDSCs in vivo.

Connective tissue growth factor (CTGF) is a cystein rich protein (Cyr61), and nephroblastoma overexpressed gene family growth factor that can promote fibroblast proliferation and matrix formation in vitro [20]. The CTGF knockout mice lead to abnormal skeletal growth with impaired chondrocyte proliferation, angiogenesis, extracellular matrix production and turnover [21]. CTGF mRNA was highly expressed during early tendon healing in a chicken flexor digitiorum profundus tendon injury model [22], which implied that CTGF might be involved in tendon repair. Treatment of human BMSCs with CTGF and ascorbic acid was reported to induce fibroblastic differentiation with increased production and mRNA expression of collagen type I and tenascin C but not osteogenic, chondrogenic and adipogenic differentiation [23,24].

Ascorbic acid, as one form of vitamin C, plays an important role in the collagen and other extracellular matrixes (ECM) production [25–27], as well as to mimic the in vivo biological microenvironment of MSCs and regulate their proliferation and differentiation [28,29]. The intraperitoneal injection of vitamin C once for every 2 days accelerated the Achilles tendon healing with early angiogenesis and increased collagen synthesis in rat model [30]. Recently, Wei et al. reported that Vitamin C alone could promote MSCs sheet formation and tissue regeneration by elevating telomerase activity [12].

In this study, we would like to test the production of engineered scaffold-free tendon tissue (ESFTT) in vitro via tenogenic differentiation of TDSCs through treatment of CTGF and ascorbic acid; and further test the hypothesis of using the ESFTT to promote tendon repair in a rat patellar tendon window injury model.

2. Materials and methods

2.1. Isolation and culture of rat GFP-TDSCs

All experiments were approved by the Animal Research Ethics Committee, the Chinese University of Hong Kong. 4-6-week-old male GFP (Green Fluorescent Protein) Sprague–Dawley rats, weighting 250–300 g were used in this study. The procedure of isolation and culture rat GFP-TDSCs was established in our previous work as illustrated in Fig. 1A [14,15]. In brief, the patellar tendons were excised from healthy rats overdosed with 2.5% sodium phenobarbital. The tissues were minced, digested with type I collagenase (3 mg/ml; Sigma–Aldrich, St Louis, MO, USA) and passed through a 70 μm cell strainer (Becton Dickinson, Franklin Lakes, USA) to yield single-cell suspension. The released cells were washed in PBS and resuspended in low glucose Dulbecco's Modified Eagle Medium (LG-DMEM) (Invitrogen Corporation, Carlsbad, USA), 10% fetal bovine serum (FBS), 100 U/ml penicillin, 100 μg/ml streptomycin and 2 mM L-glutamine (complete culture medium) (all from Invitrogen Corporation, Carlsbad, USA). The isolated cells were plated at low density (500 cells/cm^2) and cultured at 37 °C, 5% CO_2 to form colonies. At day 2 after initial

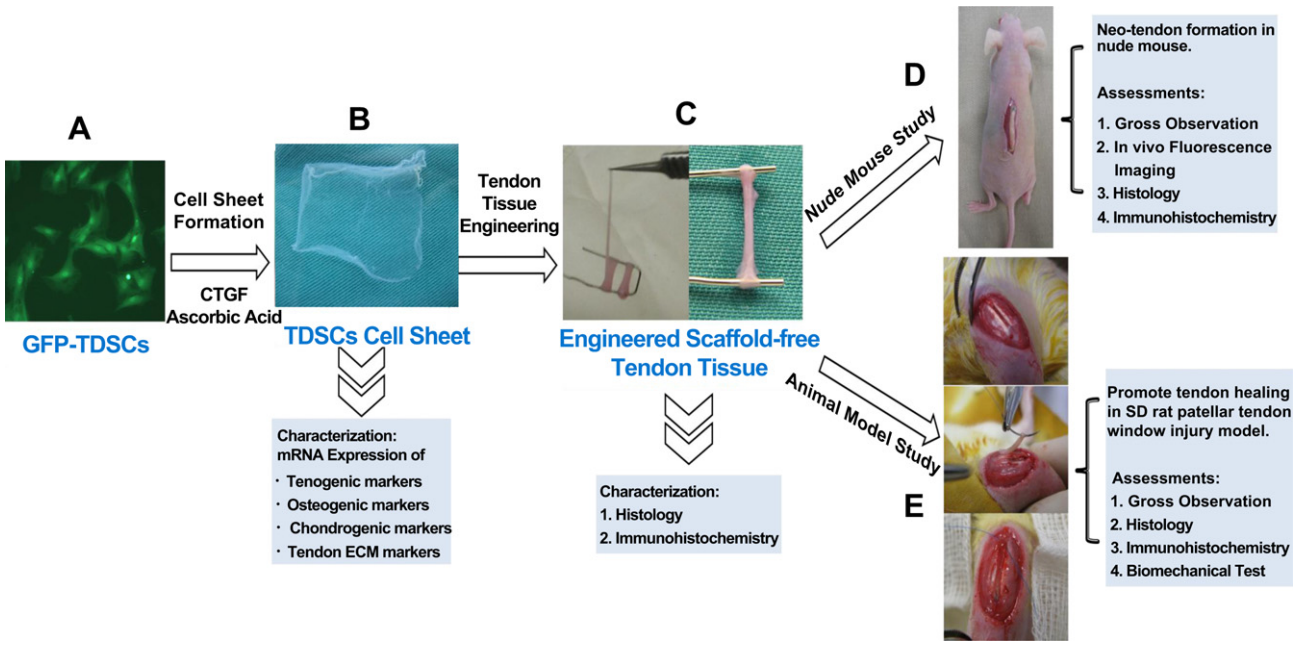

Fig. 1. The GFP-TDSCs (A) formed a cellular sheet (B) after treated by CTGF and ascorbic acid. The TDSCs cell sheet (B) was then rolled up and loaded on a 1 cm wide U-shaped spring to form engineered scaffold-free tendon tissue (C), which was sutured on the back of nude mice (D) to form neo-tendon in vivo. The engineered scaffold-free tendon tissue was sutured to the patellar bone and tibia tuberosity to promote tendon healing in a SD rat patellar tendon window injury model (E).

plating, the cells were washed twice with PBS to remove non-adherent cells. At day 7–10, they were trypsinized and mixed together as passage 0 (P0). GFP-TDSCs were sub-cultured when they reached 80–90% confluence. Medium was changed every three days. Cells at passage 4 were used for all experiments. The colongenicity and multi-differentiation potentials of the isolated cells were confirmed by colony forming assay, osteogenic, adipogenic and chondrogenic differentiation assays in vitro before being used for the experiments in this study.

2.2. In vitro engineered scaffold-free tendon tissue by using TDSCs cell sheet

GFP-TDSCs were plated at 5000 cells/cm^2 in a T75 flask and cultured in complete culture medium until the cells reached confluence. The cells were then incubated in alpha-MEM at low serum concentration (5%) with (induction group) or without (control group) the supplementation with ascorbic acid (25uM) (Catalog#A-0278, Sigma, USA) and CTGF (25 ng/ml) (Human CTGF, Catalog#120-19, PeproTech, USA) at 37 °C, 5% CO_2. Medium with or without CTGF and ascorbic acid was changed every 3 days. After treated by CTGF and ascorbic acid for 2 weeks, abundant ECM was produced by TDSCs and a cellular sheet was formed as shown in Fig. 1B. For collection of cell sheet, 1 ml 0.25% trypsin (Invitrogen Corporation, Carlsbad, USA) was added into the T75 flask and clap the flask lightly for about 20 s to detach the cell sheet, and 10 ml culture medium was added into the flask to neutralize the trypsin. The TDSCs cell sheets were collected in 10 cm cell culture dishes, then rolled up and loaded on a 1 cm wide U-shaped spring to form tendon-like structure as shown in Fig. 1C, which were used in the following studies.

2.3. Quantitative real time RT-PCR (qRT-PCR)

qRT-PCR was performed as previously described [15]. GFP-TDSCs were plated at 5000 cells/cm^2 in a 24-well plate and cultured in complete culture medium until the cells reached confluence. The cells were then incubated with ascorbic acid (25uM) and CTGF (25 ng/ml) or medium only in alpha-MEM at low serum concentration (5%) at 37 °C, 5% CO_2. Medium with or without CTGF and ascorbic acid was changed every 3 days. At week 2 after treatment, the cells were harvested for qPCR analysis of expression of Tnmd, Scleraxis (Scx), Thrombospondin-4 (Thbs4), Osteocalcin (Bglap) and Type II collagen (COL2A1), Aggrecan (Acan). The mRNA expression of major tendon extracellular matrix genes Tenascin C (TnC), Type I Collagen (COL1A1), Decorin (Dcn), Biglycan (Bgn), Fibromodulin (Fmod), and Elastin (Eln)) was also examined. The cells were harvested and homogenized for RNA extraction with RNeasy mini kit (Qiagen, Germany). The mRNA was reversely transcribed to cDNA by the First Strand cDNA kit (Promega, Madison, WI, USA). 5 μl of total cDNA of each sample were amplified in a 25 μl reaction mix using the Platinum SYBR Green qPCR SuperMix-UDG with specific primers using the ABI StepOne Plus system (all from *Applied Biosystems,* CA, USA) (Table 1). Cycling conditions were: denaturation at 95 °C for 10 min, 45 cycles at 95 °C for 20 s, optimal annealing temperature for 25 s, 72 °C for 30 s and finally at 60–95 °C with a heating rate of 0.1 °C/s. The expression of target gene was normalized to that of β-actin gene. Relative gene expression was calculated with the $2^{-\triangle CT}$ formula.

2.4. In vivo neo-tendon formation by engineered scaffold-free tendon tissue in nude mice

In order to demonstrate the engineered scaffold-free tendon tissue can form neo-tendon in vivo, a nude mouse model was applied as illustrated in Fig. 1D. Briefly, total 8 mice were used; after anesthesia, an incision was made on the dorsum and a subcutaneous pocket was created to expose posterior midline. The scaffold-free tendon tissue was sutured to posterior midline at both ends using Ethicon 6-0 suture, there was tensile strength on the tendon graft with the mice movement. At the end of 8 ($n = 4$) and 12 weeks ($n = 4$), the implanted tissues were harvested, subject to ex vivo fluorescence imaging examination, and histology for examination of vascularity and collagen fiber alignment.

2.5. In vivo fluorescence imaging

In vivo fluorescence imaging of neo-tendon at the time of sample harvest was done by IVIS 200 imaging system (Xenogen, Alameda, CA, USA) according to our previous study protocol [17]. The nude mice were terminated with overdosing 2.5% sodium phenobarbital, the tendon tissues were harvested and immediately placed in the light-tight specimen chamber of the IVIS 200 imager. Grayscale reference images were obtained with low-light illumination. Fluorescence images were then acquired in complete darkness with Fluorescent imaging model, a GFP excitation/emission filter set, 10 s exposure time, medium binning, F/Stop 8, lamp level high, field of view C; for the cooled charge-coupled device (CCD) camera, color bar: Min = 7000, Max = 30000. The pseudo-colour image (indicating light intensity, blue least and red most intense) was superimposed over the grayscale reference image to form a composite image using Living Image analysis software (v2.50, Xenogen Corporation, Alameda, CA, USA).

2.6. Patellar tendon injury and repair animal model

Ninety six Sprague Dawley male adult rats (6–8 weeks, body weight of 250–300 g) were used in this study. To create the tendon defect, the central one-third of the patellar tendon (~1 mm in width) was removed from the distal apex of the patella to the insertion of the tibia tuberosity with two stacked sharp blades according to our well-established protocol as illustrated in Fig. 1E. The operated rats were divided into 2 groups: (a) injury-only group and (b) TDSCs cell sheet group. The engineered scaffold-free tendon tissue was placed in the tendon defect and sutured to the patellar bone and tibia tuberosity using Ethicon 6-0 suture. Window injury sutured without TDSCs cell sheet was served as control. The animals were allowed to have free-cage activity until euthanasia. At week 2, 4 and 8 after surgery, six animals in each group were killed and the patellar tendons were harvested for ex vivo examination of the presence of transplanted cells by fluorescence imaging, followed

Table 1
Table showing the primer sequence, product size and annealing temperature of target genes for real time RT-PCR.

Gene	Primer nucleotide sequence	Product size (bp)	Annealing temperature	Accession no.
β-actin	5′-ATC GTG GGC CGC CCT AGG CA-3′ (forward) 5′-TGG CCT TAG GGT TCA GAG GGG-3′ (reverse)	243	52	NM_031144
Collagen type I (Col2a1)	5′-CCGGACTGTGAGGTTAGGAT-3′(forward) 5′-AACCCAAAGGACCCAAATAC-3′(reverse)	364	55	BT007205
Collagen type II (Col2a1)	5′- CATCGGTGGTACTAAC-3′(forward) 5′- CTGGATCATATTGCACA-3′(reverse)	238	55	NM_053356.1
Aggrecan (Acan)	5′-CTTGGGCAGAAGAAAGATCG-3′ (forward) 5′-GTGCTTGTAGGTGTTGGGGT-3′ (reverse)	158	58	J03485
Biglycan (Bgn)	5′- TCTACATCTCCAAGAACCACCTGG-3′ (forward) 5′- TTGGTGATGTTGTTGGAGTGCAGA-3′ (reverse)	513	55	NM_017087.1
Decorin (Dcn)	5′-ATGATTGTCATAGAACTGGGC-3′ (forward) 5′-TTGTTGTTATGAAGGTAGAC-3′ (reverse)	382	55	NM_022190.1
Fibromodulin (Fmod)	5′-GCTCTGGGCTCCTACTCCTT-3′ (forward) 5′-GTCCTGCCATTCTGAGGTGT-3′ (reverse)	450	58	NM_080698.1
Scleraxis (Scx)	5′- AACACGGCCTTCACTGCGCTG-3′(forward) 5′- CAGTAGCACGTTGCCCAGGTG-3′(reverse)	123	58	NM_001130508.1
Tenomodulin (Tnmd)	5′-CCATGCTGGATGAGAGAGGTTAC-3′(forward) 5′-CACAGACCCTGCGGCAGTA-3′(reverse)	72	58	NM_022290.1
Osteocalcin (Bglap)	5′-GGTGCAAAGCCCAGCGACTCT-3′(forward) 5′-GGAAGCCAATGTGGTCCGCTA-3′(reverse)	199	60	M23637
Tenascin C (TnC)	5′-CAGAAGCTGAACCGGAAGTTG-3′ (forward) 5′-GGCTGTTGTTGCTATGGCQCT-3′(reverse)	278	55	NM_053861.1
Elastin (Eln)	5′-AAAGTTCCTGGTGTCGGTCTTCCA-3′(forward) 5′- AGCAGCTCCATACTTAGCAGCCTT -3′(reverse)	528	62	NM_012722.1
Thrombospondin-4 (Thbs4)	5′-TCCACGTAAACACCCAGACA-3′(forward) 5′- TTCTGCTACTGCACGGAATG -3′(reverse)	140	60	XM_342172.4

by histology for the examination of cellularity and vascularity of the regenerated tissue and polarization microscopy for the assessment of collagen fiber alignment. The fate of TDSCs cell sheet in the tendon defect was followed by immunohistochemical staining of tenogenic-specific (Tenomodulin) and tendon ECM (type I and III collagen) markers. At week 2, 4 and 8, another 10 animals from each group were euthanatized and both the contralateral intact and the injured patellar tendons were harvested for biomechanical test.

2.7. Ultrasound imaging

The patellar tendon samples were scanned before the biomechanical testing by the animal ultrasound system (Vevo-770 High Resolution In-Vivo Micro-Imaging System, VisualSonics, Toronto, Ontario, Canada) according to our previous study protocol [17]. The ultrasound system is equipped with a rat handling platform, a 3-D motor, a 3-D mode imager and a RMVTM (real-time micro visualization) 711 scan head at 55 MHz. The resolution of the ultrasound system is 3.0 mm. Briefly, the harvested knee was shaved and placed on the handling platform in a supine position with knee flexion of approximately 100°. The limb was fixed with modeling clay and coupling gel was added to cover the whole knee. After determining the best position for imaging, the 3D image of the patellar tendon was scanned for 12 mm with step size of 0.032 mm. The tendon contour corresponding to the rupture site in the biomechanical test was drawn and the cross-sectional area was measured using the system software. The same operator, whom was blinded to the study groups, performed the ultrasound imaging examination in this study.

2.8. Biomechanical testing

We followed the procedures as described in previous study [17]. The patellar–patellar tendon-tibia composite was first isolated. The regenerated tissue in the window wound connected to the bony ends was then isolated by excising the medial and lateral healthy tendon using two stacked blades similar to the creation of tendon defect. The composite was fixed on a custom-made testing jig with two clamps. The lower one was used to fix the tibia shaft and plateau while the upper one was used to fix the proximal patella, the quadriceps muscles and its tendons without creating mechanical stress to the junction and the mid-substance. The whole construct was then mounted onto the Hounsfield H25KS mechanical testing machine (Tinius Olsen Ltd, *Salfords*, UK). The test to failure was performed at a testing speed of 40 mm/min and preload of 0.1N using a 50-N load cell. The load–displacement curve of the healing tendon tissue was recorded. The ultimate stress (N/mm^2) was calculated based on the ultimate load divided by the cross-sectional area at the break point measured by high-resolution Vevo 770 animal ultrasound system (Visualsonics, Toronto, Canada) with images taken immediately prior to the biomechanical test. The Young's modulus (N/mm^2) was calculated from the linear slope of a stress–strain curve. The percentage of testing values in the regenerated tissue to the central portion of the contralateral healthy patellar tendon created similarly with two stacked blades was also reported.

2.9. Histology and immunohistochemistry

The formed engineered scaffold-free tendon tissue, neo-tendon tissue and regenerated patellar tendon tissue were washed in PBS, fixed in buffered formalin and 100% ethanol, embedded in paraffin, cut longitudinally to 5-μm thick sections and mounted on 3-aminopropyl-triethoxy-silane (Sigma–Aldrich, St Louis, MO, USA) coated slides. After deparaffination, the sections were stained with hematoxylin and eosin. Immunohistochemistry was done as described previously [17,31,32]. Briefly, after deparaffination, the sections were rehydrated, quenched of endogenous peroxidase activity and subject to antigen retrieval. After blocking with 5% normal donkey and goat serum, the sections were incubated with specific antibodies against Tenomodulin, Collagen Type I & III, GFP, Osteocalcin, Collagen Type II (sc-49325, sc-8784, sc-8780, sc-8334, sc-365797, Santa Cruz Biotechnology, CA, USA; MS-235-P, Thermo Scientific, USA) at dilution of 1:100 at 4 °C overnight. Donkey anti-goat horseradish peroxidase (HRP)-conjugated secondary antibody, goat anti-rabbit horseradish peroxidase (HRP)-conjugated secondary antibody and goat anti-mouse horseradish peroxidase (HRP)-conjugated secondary antibody (sc-2020, sc-2030, sc-2302, Santa Cruz Biotechnology, CA, USA; all at a dilution sof 1:100) were then added for an hour respectively, followed by 3, 3′ diaminobenzidine tetrahydrochloride (K3468, DAKO, Glostrup, Denmark) in the presence of H_2O_2. Afterward, the sections were rinsed, counterstained in hematoxylin, dehydrated with graded ethanol and xylene, and mounted with p-xylene-bis-pyridinium bromide (DPX) permount (Sigma Aldrich, St Louis, MO, USA). Primary antibody was replaced with blocking solution in the negative controls. All incubation times and conditions were strictly controlled. Samples from nude mouse or tendon window injury studies were stained in the same batch. The sections were examined under light microscopy (DMRXA2, Leica Microsystems Wetzlar GmbH, Germany).

2.10. Data analysis

Data was presented as mean ± SD and shown in boxplots. Comparison of 2 groups at different time points was done using Mann–Whitney *U* test. All the data analysis was done using SPSS (SPSS Inc, Chicago, IL, USA; version 16.0), $p < 0.05$ was regarded as statistically significant.

3. Results

3.1. Gross observation of TDSCs cell sheet and engineered scaffold-free tendon tissue

After treated by CTGF and ascorbic acid for 2 weeks, a cellular sheet was formed by TDSCs (Fig. 1B). This TDSCs cell sheet was detached by trypsin from cell culture flask and transferred in 60 mm dish. After washed by PBS, the TDSCs cell sheet was rolled up and loaded on a 1 cm wide U-shaped spring to form engineered scaffold-free tendon tissue (Fig. 1C), which was used in following study.

3.2. Components analysis of TDSCs cell sheet and engineered scaffold-free tendon tissue

3.2.1. Tenogenic, osteogenic and chondrogenic specific markers mRNA expression in TDSCs cell sheet

The TDSCs treated by CTGF and ascorbic acid significantly increased mRNA expression of tendon-specific markers Tnmd ($p = 0.006$) (Fig. 2A), Scx ($p = 0.006$) (Fig. 2B) and Thbs4 ($p = 0.006$) (Fig. 2C); meanwhile, the mRNA expression of chondrogenic markers Col2A1 ($p = 0.004$) (Fig. 2D), Acan ($p = 0.004$) (Fig. 2E) and osteogenic marker Bglap ($p = 0.018$) (Fig. 2F) were all significantly decreased.

3.2.2. Tendon ECM related markers mRNA expression in TDSCs cell sheet

The tendon extracellular matrix related markers Col1A1 ($p = 0.004$) (Fig. 2G), Eln ($p = 0.004$) (Fig. 2I), Dcn ($p = 0.004$) (Fig. 2J), Bgn ($p = 0.004$) (Fig. 2K) were also significantly increased in TDSCs after treatment of CTGF and ascorbic acid. The induction group had higher mRNA expression of TnC (Fig. 2H) than the control group without significant difference ($p = 0.078$). There was no significant difference for the Fmod (Fig. 2L) mRNA expression in TDSCs after treated by CTGF and ascorbic acid.

3.3. Histological characteristics and tendon specific markers expression in engineered scaffold-free tendon tissue

H&E staining of this engineered scaffold-free tendon tissue showed an immature tissue structure with relatively loose extracellular matrix (Fig. 3A). Polarization microscopy also confirmed that the collagen fibrils were thin and randomly oriented (Fig. 3B), with relatively higher cellularity (Fig. 3C). The GFP-TDSCs were in round, ellipse or spindle shape and randomly oriented along within the extracellular matrix (Fig. 3D). Immunohistochemistry staining for tenomodulin (Fig. 3F), collagen type I (Fig. 3G), collagen type III (Fig. 3H), GFP (Fig. 3N), collagen type II (Fig. 3O) and osteocalcin (Fig. 3P) were performed, and the intact patellar tendon was used as a control (Fig. 3J–L,R–T). The engineered scaffold-free tendon tissue group had stronger expression of tenomodulin (Fig. 3F); stronger expression of collagen type I (Fig. 3G) comparing to that in intact patellar tendon (Fig. 3J and K); the collagen type III expression was similar in the two groups (Fig. 3H,L). The TDSCs was still present in the wound areas as shown by positive staining of GFP (Fig. 3N), whereas no GFP expression in the intact patellar tendon (Fig. 3R). The engineered scaffold-free tendon tissue group had weak expression of collagen type II (Fig. 3O) and osteocalcin (Fig. 3P), with similar staining to those of the intact healthy patellar tendon (Fig. 3S,T).

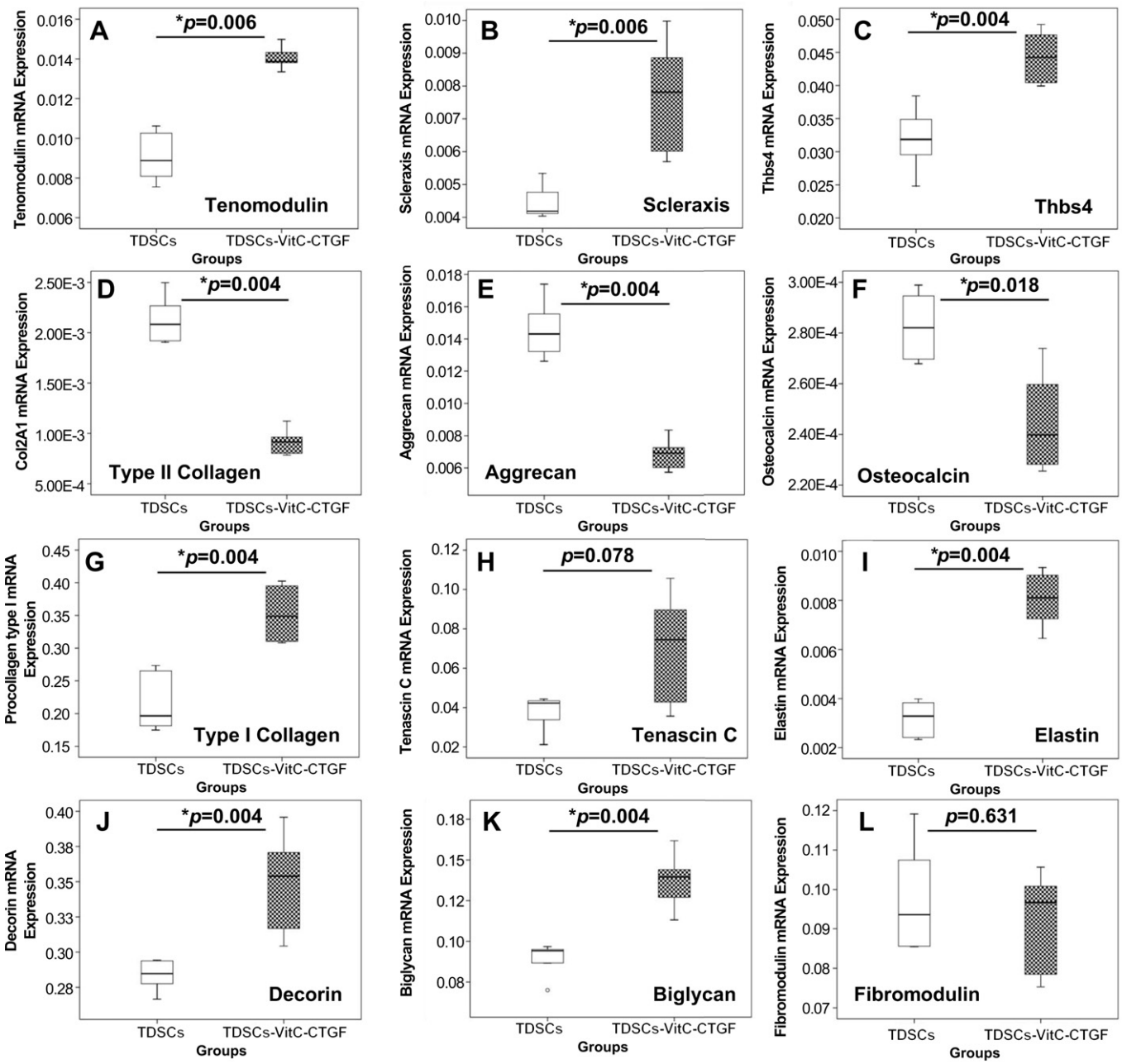

Fig. 2. Boxplots showing the mRNA expression of (A) Tenomodulin; (B) Scleraxis; (C) Thbs4; (D) Type II Collagen; (E) Aggrecan; (F) Osteocalcin; (G) Type I Collagen; (H) Tenascin C; (I) Elastin; (J) Decorin; (K) Biglycan; (L) Fibromodulin after treatment of GFP-TDSCs with and without ascorbic acid (25uM) and CTGF (25 ng/ml) for 2 weeks. $^{*}p < 0.05$, $N = 6$, NPar Tests, Mann–Whitney Test.

3.4. Neo-tendon formation after engineered scaffold-free tendon tissue implantation in nude mice

3.4.1. Gross observation and in vivo fluorescence imaging of neo-tendon tissues

To determine the effect of engineered scaffold-free tendon tissue on neo-tendon formation in vivo, the engineered scaffold-free tendon tissue was implanted into the nude mice. The implanted tendon tissue became slightly smaller, shorter and thinner at the end of week 8 and 12 following implantation, the gross samples were surrounded by blood vessels (Fig. 4A,B). As shown in (Fig. 4C,D), the GFP signals could be detected in all time points. The in vivo fluorescent imaging showed that the GFP-TDSCs in implanted scaffold-free tendon tissue were in situ without going to other place (Fig. 4C,D) at 8 and 12 weeks in nude mice.

3.4.2. Histology of neo-tendon tissue

After 8 weeks transplantation, there were loosely deposited collagens in the tendon-like structure (Fig. 4E,F), the collagen fibrils became mature at 12 weeks (Fig. 4G,H). Elongated or spindle-shaped TDSCs were longitudinally aligned along with collagen fibers with time development (Fig. 4E,G). More extracellular matrices and collagen were produced at 12 weeks (Fig. 4G,H) than that of 8 weeks (Fig. 4E,F). At week 8, the collagen birefringence was weak (Fig. 4F); it increased at 12 week (Fig. 4H). At week 12, D-band periodicity representing tendon structure was

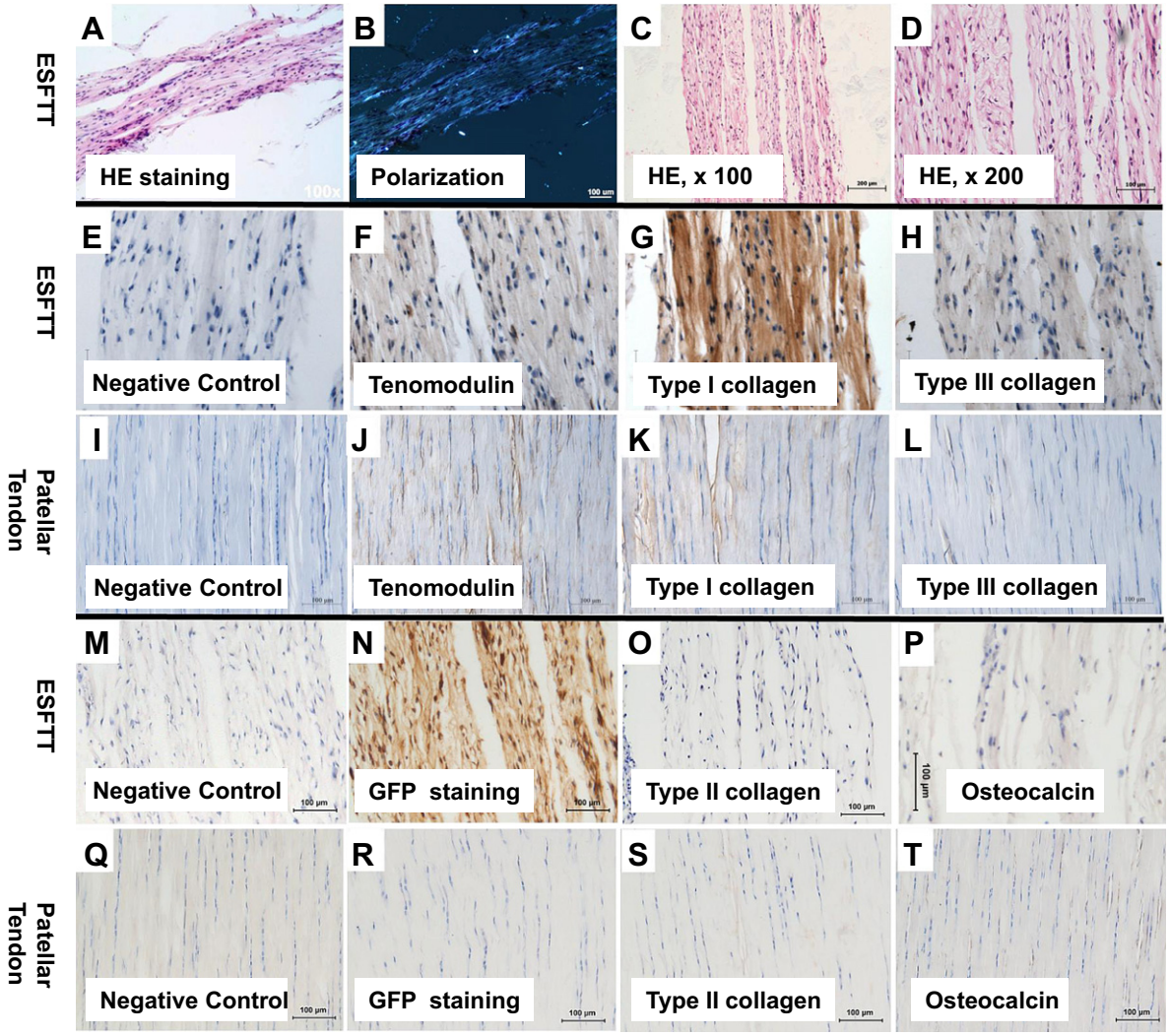

Fig. 3. Photographs showing histology (A–D) and immunohistochemistry (E–T) investigation of engineered scaffold-free tendon tissue. Photomicrographs showing the collagen fiber alignment shown by polarization microscopy (A, B) and the H&E staining of this engineered scaffold-free tendon tissue (100x, C; 200x, D). (E) Negative control of immunostaining of the engineered scaffold-free tendon tissue; (F) Tenomodulin expression in engineered scaffold-free tendon tissue; (G) Collagen type I expression in engineered scaffold-free tendon tissue; (H) Collagen type III expression in engineered scaffold-free tendon tissue; (I) Negative control of immunostaining of intact patellar tendon; (J) Tenomodulin expression in intact patellar tendon; (K) Collagen type I expression in intact patellar tendon; (L) Collagen type III expression in intact patellar tendon. (M) Negative immuostaining control of engineered scaffold-free tendon tissue; (N) GFP expression in engineered scaffold-free tendon tissue; (O) Collagen type II expression in engineered scaffold-free tendon tissue; (P) Osteocalcin expression in engineered scaffold-free tendon tissue; (Q) Negative control of immunostaining in intact patellar tendon; (R) GFP expression in intact patellar tendon; (S) Collagen type II expression in intact patellar tendon; (T) Osteocalcin expression in intact patellar tendon. Stains: Hematoxylin and eosin (A–D), immunohistochemistry staining for Tenomodulin (F, J), Collagen type I (G, K), Collagen type III (H, L), GFP (N, R), Collagen type II (O, S) and Osteocalcin (P, T); magnification: 100× (A–C), 200× (D, E-T), scale bar: 100 μm (D, E-T), 200 μm (A–C).

observed in the wounded area under polarization microscopy (Fig. 4H', arrows).

3.5. Immunohistochemistry staining results of the neo-tendon tissues

Immunohistochemistry staining for tenomodulin, collagen type I, collagen type III, GFP, collagen type II and osteocalcin was performed in the neo-tendon tissues at 8 and 12 weeks following implantation, and in the normal patellar tendon (as control). At week 8, the tenomodulin expression in the neo-tendon was weaker than that of week 12 (Fig. 5A2,B2); the collagen type I immunostaining showed no difference between week 8 and 12 (Fig. 5A3, B3); the collagen type III expression was stronger at week 8 than that of week 12 (Fig. 5A4, B4). At week 12, the staining patterns of tenomodulin, collagen type I and collagen type III were similar to that of intact patellar tendon (Fig. 5B2–4, C2–4). The GFP immunostaining was positive at week 8 and 12, but the GFP expression was stronger at week 8 than that of week 12 (Fig. 5D2,E2). The intact patellar tendon had no expression of GFP (Fig. 5F2). At week 12, the neo-tendon did not express collagen type II and osteocalcin, similar was true in the intact patellar tendon (Fig. 5G2,3, H2,3). No positive signal was found in any of the negative control groups (Fig. 5A1,B1,C1,D1,E1,F1,G1, and H1).

3.6. Promote tendon healing by scaffold-free tendon tissue in rat patellar tendon injury model

3.6.1. Gross observation

At the first 2 weeks post-operation, all the skin incision wounds healed with no sign of infection, swelling and suppuration. During the last 6 weeks post-operation, no apparent difference was

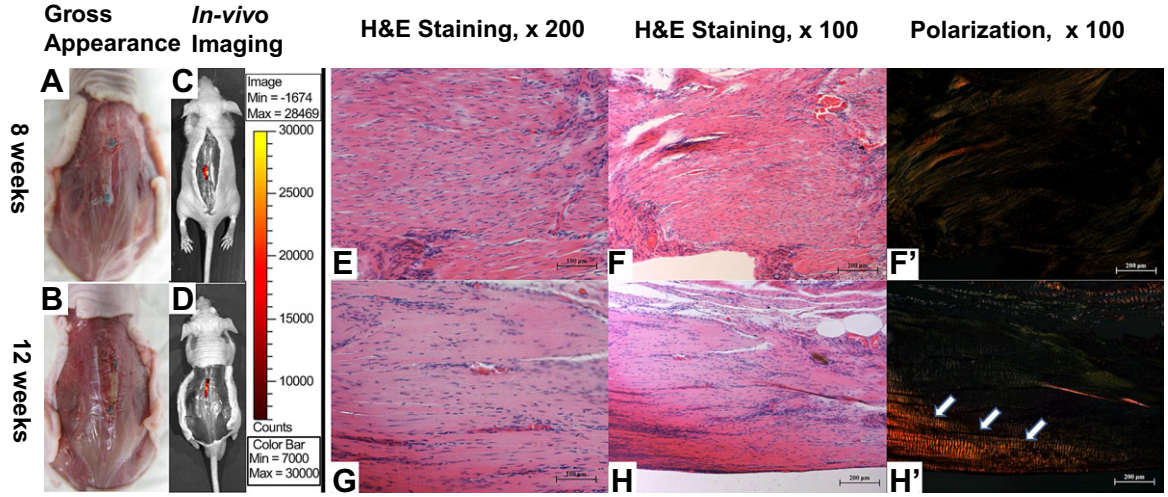

Fig. 4. Photographs show gross observation and in vivo fluorescence imaging of the neo-tendon in nude mice. (A) Gross observation at week 8 after implantation; (B) Gross observation at week 12 after implantation; (C) in vivo fluorescence imaging at week 8 after implantation; (D) in vivo fluorescence imaging at week 12 after implantation. The H&E staining (E, G) and polarization microscopy (F, F', H, H') of neo-tendon tissue formation by engineered scaffold-free tendon tissue at week 8 (E, F, F') and week 12 (G, H, H') in the nude mice. Stains: Hematoxylin and esoin; Magnification: 100× (F, F', H, H'), 200× (E, G), scale bar: 100 μm (E, G), 200 μm (F, F', H, H').

noticed in animals in all groups. The vascularity in the ESFTT group was lower than that of control group at week 2. The vascularity decreased at week 4 and week 8 in both groups. The injury gap was observed in both groups at 2 weeks but became less clear at 4 and 8 weeks. After resecting the intact patellar tendon tissue around the injury gap, the regenerated patellar tendon tissue looked tough and thick in the ESFTT group, having similar appearance as the intact patellar tendon (Fig. 6B1–3), whereas the regenerate tissues still looked transparent and thin in the control group at 4 and 8 weeks (Fig. 6A1–3).

3.6.2. Histology and polarization microscopy

Both the ESFTT group and control group have higher cellularity at week 2 (Fig. 6C1,D1) in the wounded area compared to the region outside the window injury, but the ESFTT group appeared to have higher cellularity in the injury window region than that of the control group (Fig. 6D1). The cellularity in both groups reduced, with some extracellular matrix deposition at week 4 (Fig. 6C2,D2, arrow) and week 8 (Fig. 6C3,D3, arrow), and the extracellular matrix production in ESFTT group (Fig. 6D1–3, arrow) was obviously more than that of control group (Fig. 6C1–3, arrow) at all time points, as shown by the Eosin staining intensity of the extracellular matrix. The healing tendon cells in the control group were round and randomly oriented at week 2 and 4 (Fig. 6C1,2, *), but some cells became more elongated at week 8 (Fig. 6C3, *). Most of the healing tendon cells were round and randomly oriented at week 2 in the ESFTT group, similar to that in the control group, but some cells were already elongated even at week 2 (Fig. 6D1, *). At week 4 and 8, more and more healing tendon cells became longitudinally-arranged spindle-shaped and were embedded between parallel collagen fibers (Fig. 6D2,3, *).

The collagen birefringence was low at week 2 and increased with time in both groups (Fig. 6E1-3, E1-3', F1-3, F1'-3'). Higher collagen birefringence was observed at week 2 and week 4 in the ESFTT group compared to that in the control group, indicating better collagen fiber alignment (Fig. 6E1' vs. F1' and Fig. 6E2' vs. F2'). At week 8, collagen fibers with D-band periodicity, typical of tendon structure, was observed in the ESFTT group, but not in the control group (Fig. 6E3' vs. F3'). No fibrocartilage or ectopic bone was observed in both groups up to week 8.

3.6.3. Tendon specific ECM markers expression in the regenerated tendon tissue

Immunohistochemistry staining for tenomodulin, collagen type I and collagen type III was performed in the regenerated tendon tissue at 2, 4 and 8 weeks. The expression of tenomodulin in the control group was the strongest at week 4 (Fig. 7A3) than that of week 2 and 8 (Fig. 7A2,A4); however, the tenomodulin expression in the ESFTT group was the strongest at week 2, and decreased at week 4 and 8 gradually (Fig. 7B2–4). In both groups, the expression of collagen type I was positive at week 2 (Fig. 7C2,D2), reduced at week 4 (Fig. 7C3,D3), and became weaker in both groups at week 8 (Fig. 7C4,D4). The expression of collagen type III was weak in the ESFTT group at all time points (Fig. 7F2–4), but in the control group, the expression of collagen type III increased with time (Fig. 7E2–4). No positive signal was detected in all the negative controls for immunostaining (Fig. 7A1,B1,C1,D1,E1,F1).

3.6.4. Osteogenic and chondrogenic markers expression in the neo-tendon tissues

At week 8, the osteocalcin expression was positive in the control group (Fig. 8A2) whereas negative in the ESFTT group (Fig. 8B2); the collagen type II was negatively expressed with no difference between the control group (Fig. 8A3) and the ESFTT group (Fig. 8B3). There was no positive signal in all the negative controls (Fig. 8A1,B1).

3.6.5. The fate of the transplanted engineered scaffold-free tendon tissues

The fate of the transplanted GFP-TDSCs was traced with ex vivo fluorescent imaging of the GFP signals, and was double checked by immunohistochemistry staining of GFP. The immunostaining of GFP results showed that the GFP expression was positive at week 2, 4 and 8, but it was reduced at week 4 and 8 with time (Fig. 8D2–4). The expression of GFP was negative in the control group at all time points. No positive signal was detected in all the negative controls (Fig. 8A1,B1,C1,D1). The ex vivo fluorescent imaging results showed that the transplanted GFP positive cells were present in the window wound in the ESFTT group at week 2 (Fig. 8F1). However, the GFP signal decreased and became almost undetectable at week 4 and 8 (Fig. 8F2,3), and only one sample in the ESFTT group showed some

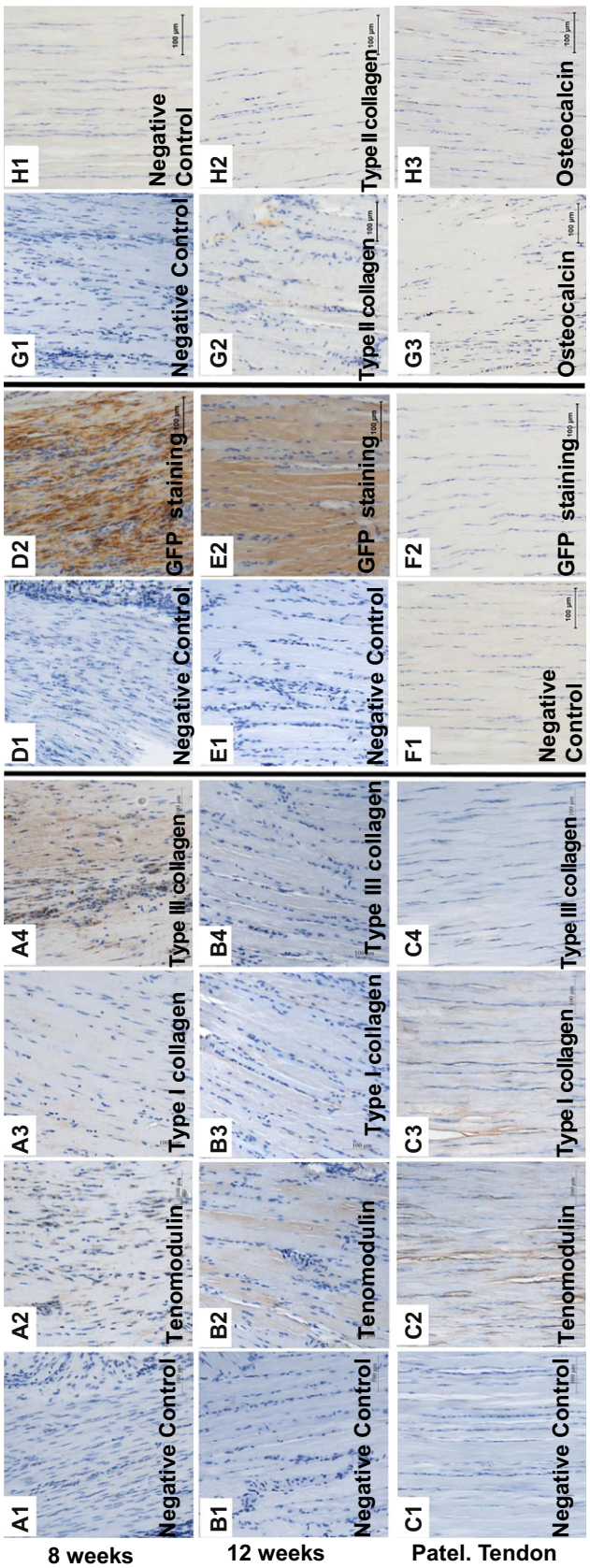

Fig. 5. Photomicrographs show the immunohistochemistry staining for Tenomodulin (A2, B2, C2), Collagen type I (A3, B3, C3), Collagen type III (A4, B4, C4), GFP (D2, E2, F2), Collagen type II (G2, H2) and Osteocalcin (G3, H3) in the neo-tendon tissue formed at week 8 (A1–4, D1–2), 12 (B1–4, E1–2, G1-3, H1-3) and intact patellar tendon (C1–4, F1–2). A1, B1, C1, D1, E1, F1, G1, H1 are negative controls for immunostaining. Magnification: 200×, scale bar: 100 μm.

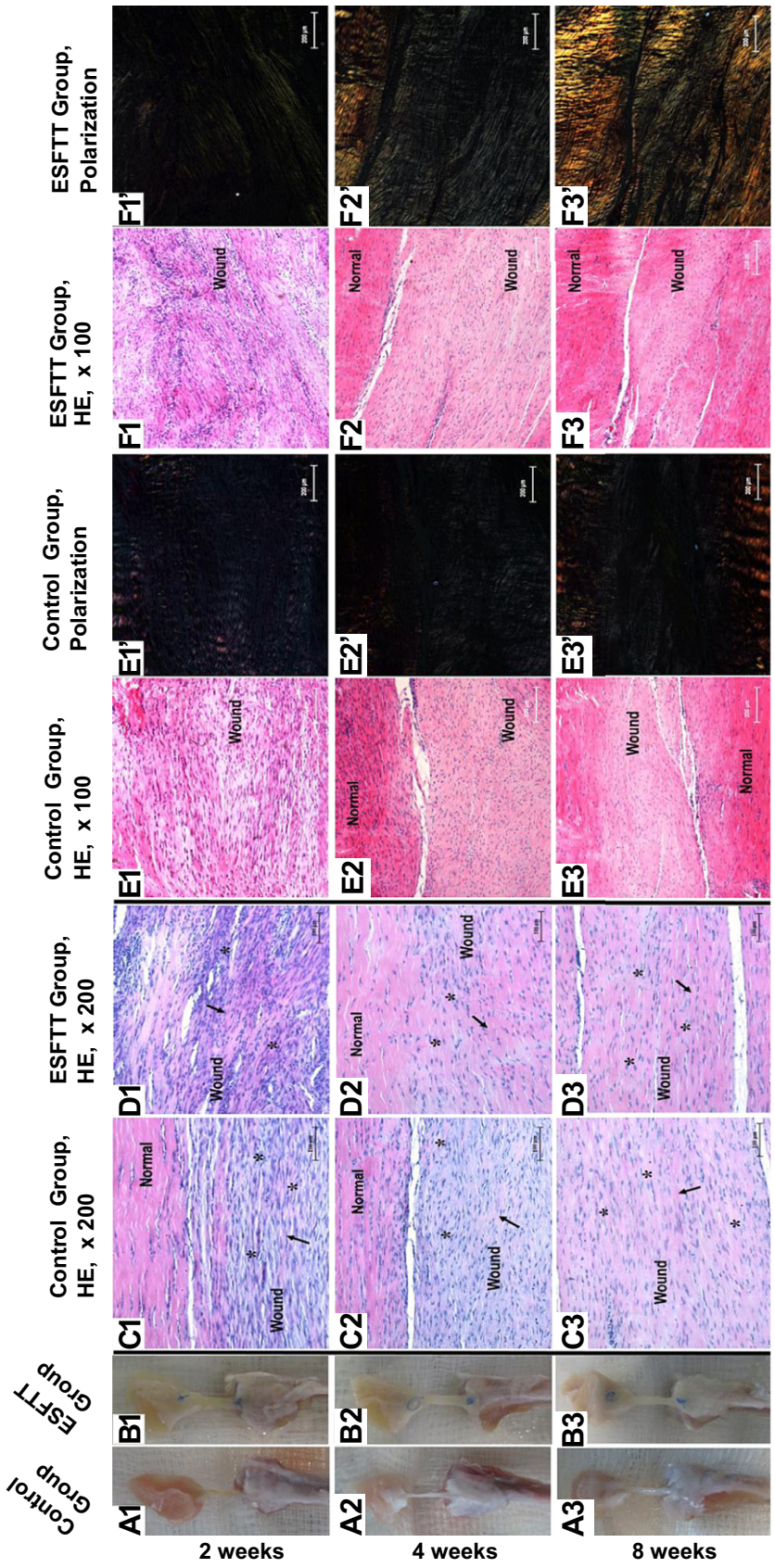

Fig. 6. Photographs show the gross view of the patellar tendon in the control group (A1-3) and ESFTT group (B1-3) at week 2 (A1, B1), week 4 (A2, B2) and week 8 (A3, B3) after healing. Photomicrographs show the H&E staining of the window defect in the control group (C1-3) and the ESFTT group (D1-3) at week 2 (C1, D1), 4 (C2, D2) and 8 (C3, D3) after repair. Photomicrographs show the histology (E1-3, F1-3) and the corresponding polarized image (E1'-3', F1'-3') in the window defect in the control group (E1-3, E1'-3') and ESFTT group (F1-3, F1'-3') at week 2 (E1, E1', F1, F1'), week 4 (E2, E2', F2, F2'), week 8 (E3, E3', F3, F3') after repair. Stains: Hematoxylin and eosin; Arrows: collagen fibers; *: healing tendon cells. Magnification: 100× (E1-3, E1'-3', F1-3, F1'-3'), 200x (C1-3, D1-3). Scale bar: 100 μm (C1-3, D1-3), 200 μm (E1-3, E1'-3', F1-3, F1'-3').

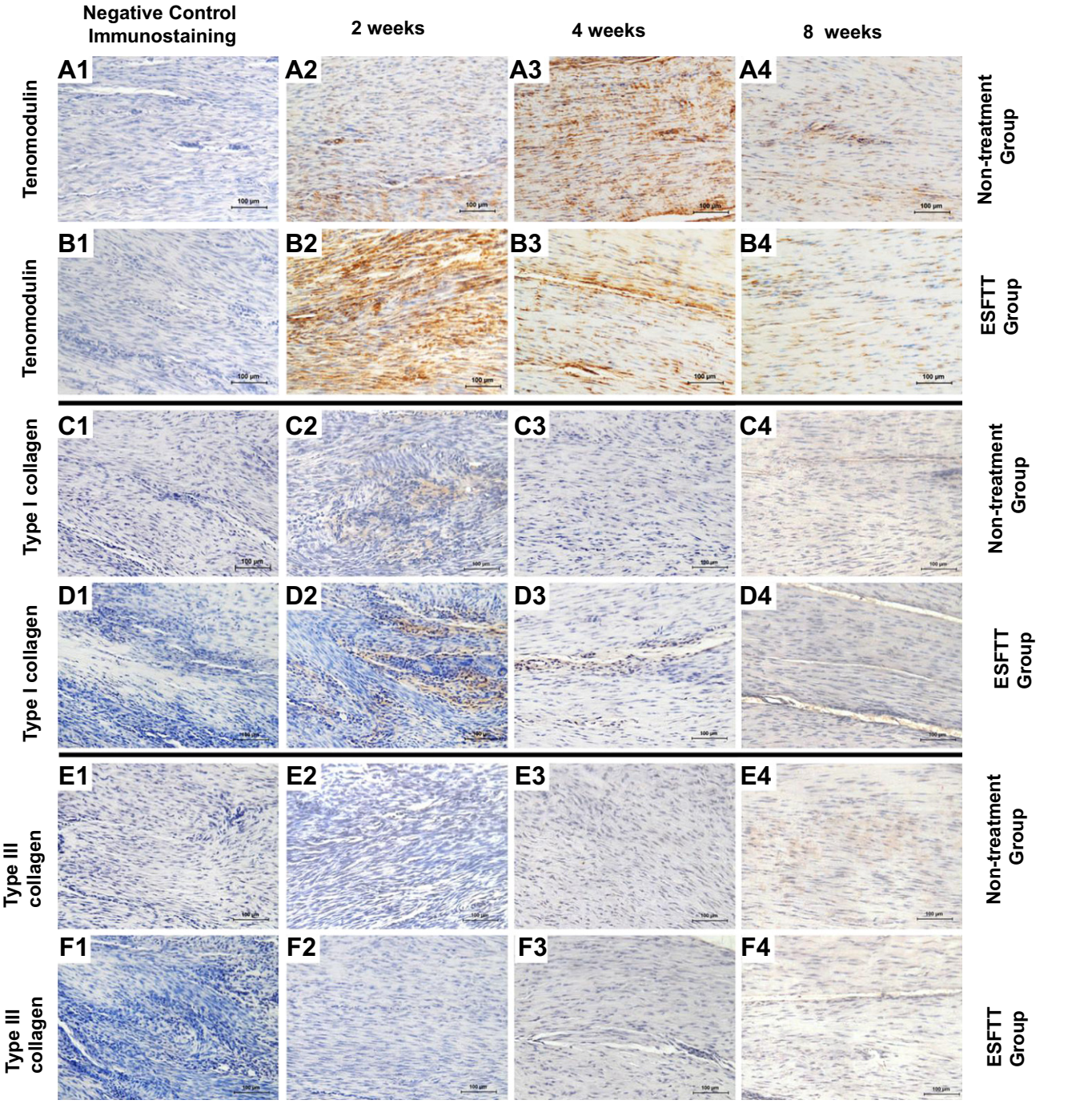

Fig. 7. Photomicrographs show the immunohistochemistry stainings for Tenomodulin (A2-4, B2-4), Collagen type I (C2-4, D2-4) and Collagen type III (E2-4, F2-4) of regenerated tendon tissue formation by tissue engineering tendon at week 2 (A2, B2, C2, D2, E2, F2), week 4 (A3, B3, C3, D3, E3, F3) and week 8 (A4, B4, C4, D4, E4, F4) in the SD rat patellar tendon window injury. A1, B1, C1, D1, E1, F1 are negative controls for immunostaining. Magnification: 200×, scale bar: 100 μm.

weak signal at week 4. No fluorescent signal was detected in the control group at all time points (Fig. 8E1–3).

3.6.6. Biomechanical testing

The ultimate stress was significantly higher in the TDSCs cell sheet group compared to that in the control group at all time point (2wk: $p = 0.012$, 5.38 ± 2.31 N/mm^2 versus 12.35 ± 3.62 N/mm^2; 4wk: $p = 0.01$, 10.73 ± 2.61 N/mm^2 versus 23.18 ± 7.96 N/mm^2; 8wk: $p = 0.001$, 18.42 ± 4.01 N/mm^2 versus 29.21 ± 4.40 N/mm^2) (Fig. 9A). The Young's modulus was significantly higher in the TDSCs cell sheet group compared to that in the control group at all time point (2wk: $p = 0.004$, 36.90 ± 14.85 N/mm^2 versus 99.72 ± 12.10 N/mm^2; 4wk: $p = 0.004$, 76.83 ± 16.93 N/mm^2 versus 132.84 ± 35.59 N/mm^2; 8wk: $p = 0.001$, 128.28 ± 11.25 N/mm^2 versus 183.45 ± 14.66 N/mm^2) (Fig. 9B).

At week 2, TDSCs cell sheet implantation restored the ultimate stress to $35.92\% \pm 10.29\%$ of the contralateral control compared to only $17.23\% \pm 7.62\%$ in the control group ($p = 0.004$), and restored the Young's modulus to $46.92\% \pm 9.60\%$ of the contralateral control compared to only $18.04\% \pm 7.40\%$ in the control group ($p = 0.004$).

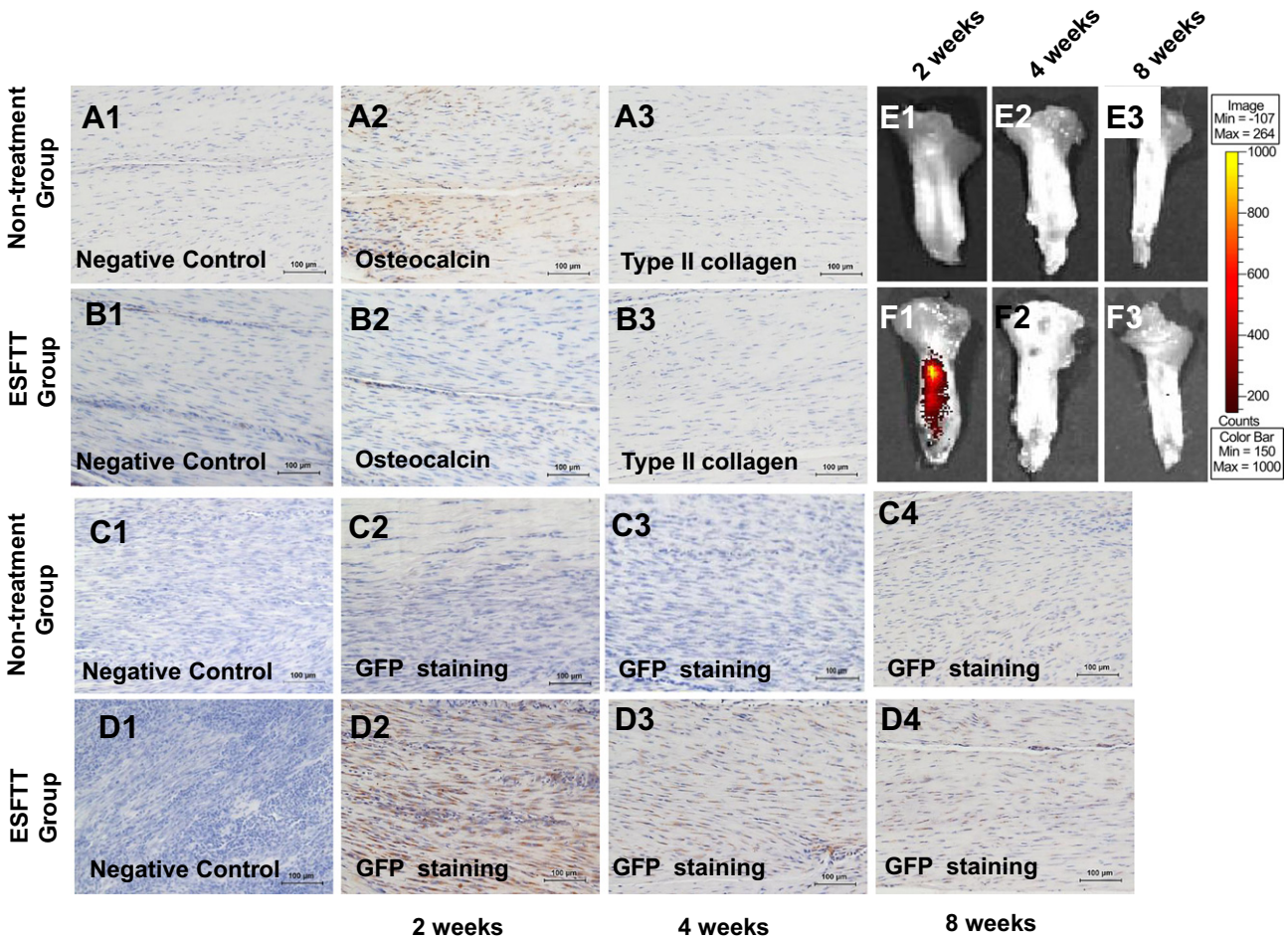

Fig. 8. Photomicrographs show the immunohistochemistry staining for Osteocalcin (A2, B2) and Collagen type II (A3, B3) in regenerated tendon tissues in the control group and the ESFTT group at week 8; and the immunostaining for GFP in the regenerated tendon tissue in the control group (C2-4) and the ESFTT group (D2-4) at week 2 (C2, D2), 4 (C3, D3) and 8 (C4, D4) in the SD rat patellar tendon window injury model. A1, B1, C1, D1 are negative controls for immunostaining. Magnification: 200×, scale bar: 100 μm. Photographs show ex *vivo* fluorescence imaging of regenerated tendon tissue in the control group (E1-3) and the ESFTT group (F1-3) at week 2 (E1, F1), week 4 (E2, F2) and week 8 (E3, F3) in the SD rat patellar tendon window injury model.

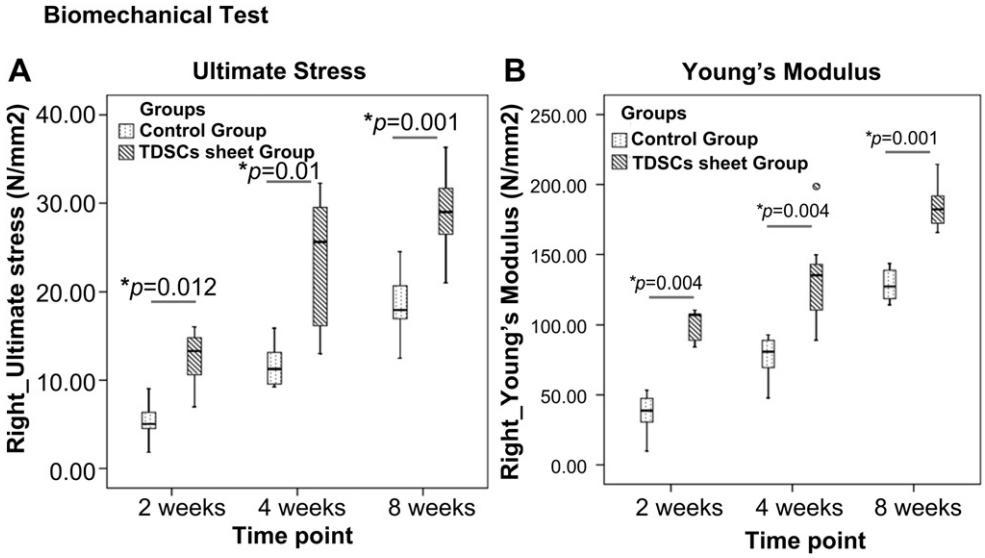

Fig. 9. Boxplots show (A) the ultimate stress and (B) the Young's modulus in the control group and the ESFTT group at week 2, 4 and 8 after repair. $^{*}p \leq 0.05$, Mann–Whitney *U*-test.

At week 4, TDSCs cell sheet implantation restored the ultimate stress to 62.37% ± 15.54% of the contralateral control compared to only 36.60% ± 7.90% in the control group ($p = 0.01$), and restored the Young's modulus to 72.59% ± 11.90% of the contralateral control compared to only 32.09% ± 8.28% in the control group ($p = 0.003$). At week 8, TDSCs cell sheet implantation restored the ultimate stress to 81.12% ± 9.94% of the contralateral control compared to only 55.46% ± 10.91% in the control group ($p = 0.003$), and restored the Young's modulus to 91.11% ± 3.74% of the contralateral control compared to only 62.00% ± 8.80% in the control group ($p = 0.001$).

4. Discussion

In this study, we successfully constructed engineering scaffold-free tendon tissue using TDSCs cell sheet in vitro, which was formed by TDSCs with the tenogenic induction of ascorbic acid and CTCF, and the neo-tendon was formed in vivo after transplantation in a nude mouse model. Furthermore, the engineered scaffold-free tendon tissue promoted tendon healing in a rat patellar tendon window injury model. The TDSCs cell sheet had increased tendon specific markers mRNA expression, decreased osteogenic and chondrogenic markers mRNA expression, as well as increased tendon ECM related markers mRNA expression. The in vitro engineered scaffold-free tendon tissue had positive protein expression of tenomodulin, collagen type I and collagen type III. The GFP-TDSCs can survive in the formed neo-tendon tissue at least for 12 weeks. This neo-tendon tissue had tendon tissue characteristics including collagen fibril polarization and tendon specific proteins (tenomodulin, collagen type I and collagen type III) expression, which were similar with that of intact healthy patellar tendon. In rat patellar tendon injury model, our ESFTT recovered histological structure and biomechanical properties of injured patellar tendon, which indicated that ESFTT had the potential to promote tendon repair.

It has been almost two decades since Langer and Vacanti reported tissue engineering to the development of functional substitutes for damaged tissue [33]. However, traditional scaffold-based tissue engineering techniques have limitations including low cell proliferation and differentiation efficiency, poor biocompatibility, biodegradable abilities, and biomechanical properties. In contrast, the cell sheet preserved cellular connections, ECM, and microenvironments, which may be a suitable biomaterial for tissue regeneration [12]. Cell sheet engineering had been applied for tissue regeneration as an alternative biomaterial in corneal, myocardial, hepatic, and periodontal tissues repair with good outcomes [34–37]. In tendon tissue regeneration, application of cell sheet engineering has not been reported yet.

Our results showed that the TDSCs cell sheet was formed in vitro by the tenogenic differentiation through ascorbic acid and CTGF treatments, resulting in increase in mRNA and protein expression of tenogenic markers and major tendon-related extracellular matrix proteins. Ascorbic acid and CTGF treatment had significantly increased the expression of tenogenic markers (*Scleraxis, Tenomodulin, Thbs4*) and tendon extracellular matrix markers (*Type I collagen, Elastin, Decorin and Biglycan*). Our results therefore confirmed the tenogenic effects of CTGF and ascorbic acid on TDSCs. We also tested the expression of osteogenic and chondrogenic markers in TDSCs with and without ascorbic acid and CTGF stimulation, and showed that the expressions of osteogenic (*Osteocalcin*) and chondrogenic (*Type II collagen, Aggrecan*) markers were reduced in the TDSCs following ascorbic acid and CTGF stimulation, indicating that the TDSCs had differentiated toward the tenogenic, but not chondrogenic or osteogenic lineages. Our finding was consistent with previous studies that CTCF increased collagen type I and tenascin-C contents but not GAG content and calcium deposition in BMSCs [23]. Our results also confirmed the combined effect of ascorbic acid and CTGF on TDSCs increased protein expression of tenomodulin, type I collagen and type III collagen, which provided suitable microenvironments for promoting tenogenic differentiation. Pretreatment of TDSCs with CTGF and ascorbic acid therefore helped to TDSCs differentiating toward tenogenic lineage and forming cell sheets.

One of the major difficulties in studying the tenogenic differentiation of stem cells is the lack of clearly defined tenogenic biomarkers. Recently, *Tnmd* [38,39], *Scx* [40,41] and *Thbs4* [38] were identified as more specific markers for tendon tissue and our in vitro study also showed increased expression of these genes in TDSCs after CTGF and ascorbic acid treatment. After treatment with CTGF and ascorbic acid for 2 weeks, the TDSCs formed an elastic cell sheet with abundant extracellular matrices production. The TDSCs cell sheet was then rolled up and loaded on a 1 cm wide U-shaped spring to form the ESFTT. After transplantation of the ESFTT into nude mice for 8 and 12 weeks, neo-tendon tissues were formed with better collagen fibril alignment and more spindle shaped cells. Since the ESFTT was sutured on the middle line of the back in the mice, and they were under physiologically mechanical loading (tensile stretching) when mice move. The role of mechanical loading on the functional development and maturation of neo-tendon tissue has also been reported in previous in vitro studies [42–45]. Cyclic tensioning of decellularized human umbilical veins seeded with MSCs embedded in collagen type I hydrogel was reported to increase the cell number, resulted in parallel orientation of collagen fibers and spindle-shaped nuclei similar to native tendons as well as produced mechanically stronger constructs comparing to un-tensioned samples [45]. As we had observed, more collagens had been deposited and the collagen fibrils were more mature after transplantation in vivo, and the expression of tenomodulin, collagen type I and collagen type III were similar to that of intact healthy patellar tendon after 12 weeks implantation.

Our result showed that ESFTT could significantly enhance tendon healing through enhancing extracellular matrices production, improvement of collagen fiber alignment and increase in the biomechanical properties of the regenerated tendon tissues. The significant improvement of healing was observed as early as week 2 post-surgery and was maintained up to week 8 post-surgery. We did not find any sign of fibrocartilage or ectopic bone formation in both control and ESFTT groups up to week 8 post-surgery, suggesting the use of ESFTT was safe. The ultimate stress was significantly higher in the ESFTT group compared to that of the TDSCs group at week 4. At week 4 post-surgery, The ESFTT group restored the ultimate stress to 62.37% ± 15.54% of the contralateral intact patella; whereas the TDSCs group had reached to 48.53% ± 10.12% ($p = 0.028$). Taking together the data of histology and biomechanical testing, the ESFTT group had better healing outcome than that of TDSCs in fibrin glue group.

MSCs seeded in different scaffolds have been reported to repair and regenerate injured tendons after transplantation into animal models [18,46–50]. However, the use of these natural and synthetic polymers for cell delivery have some limitations such as inferior biocompatibility and biodegradability; poor mechanical strength and immunogenicity as well as micro-architecture of the scaffold which could affect the survival, proliferation and differentiation of the transplanted cells. The secretion of ECM by TDSCs after treatment with CTGF and ascorbic acid avoids the need of transplanting the cells with biomaterials or scaffolds. Moreover, by forming a preliminary tendon tissue structure first in vivo through cell sheets, the ESFTT had gained certain mechanical properties that are in favor of their in vivo implantation and early bearing of mechanical loading. In the present study, we didn't measure the

mechanical properties of ESFTT and neo-tendon tissues, which are needed in the future studies. We also need to further investigate the healing mechanisms of ESFTT in tendon repair and compare the use of ESFTT with other traditional tendon scaffolds in tendon repair and regeneration.

5. Conclusion

CTGF and ascorbic acid treatment significantly enhanced the tenogenic differentiation of TDSCs, and inhibited their osteogenic and chondrogenic differentiation. Treatment of TDSCs with CTGF and ascorbic acid for 2 weeks could lead to formation of elastic cell sheets, which could be used to construct ESFTT in vitro. After transplantation in nude mice for 12 weeks, the ESFTT formed neo-tendon tissues. The ESFTT have also been shown to promote tendon healing in a rat patellar tendon injury model. In conclusion, this is a proof-of-concept study demonstrating that ESFTT could be a potentially new approach for tendon repair and regeneration.

Acknowledgment

The authors would like to thank Dr. Pauline Po-Yee Lui for her useful discussion and supports for this project. This work was supported by equipment/resources donated by the Hong Kong Jockey Club Charities Trust to Kai-Ming Chan. These works were also supported in part by the National Basic Science and Development Program, PR China (973 Program, 2012CB518105); and Hong Kong Government Research Grant Council, General Research Fund (Grant No: CUHK460710) to Kai-Ming Chan.

References

[1] Maffulli N, Wong J, Almekinders LC. Types and epidemiology of tendinopathy. Clin Sports Med 2003;22:675–92.
[2] Pennisi E. Tending tender tendons. Science 2002;295:1011.
[3] Bhandari M, Guyatt GH, Siddiqui F, Morrow F, Busse J, Leighton RK, et al. Treatment of acute Achilles tendon ruptures: a systematic overview and metaanalysis. Clin Orthop Relat Res 2002;400:190–200.
[4] Leppilahti J, Puranen J, Orava S. Incidence of Achilles tendon rupture. Acta Orthop Scand 1996;67:277–9.
[5] Butler DL, Juncosa-Melvin N, Boivin GP, Galloway MT, Shearn JT, Gooch C, et al. Functional tissue engineering for tendon repair: a multidisciplinary strategy using mesenchymal stem cells, bioscaffolds, and mechanical stimulation. J Orthop Res 2008;26:1–9.
[6] Miyashita H, Ochi M, Ikuta Y. Histological and biomechanical observations of the rabbit patellar tendon after removal of its central one-third. Arch Orthop Trauma Surg 1997;116:454–62.
[7] Evans RB. Managing the injured tendon: current concepts. J Hand Ther 2012; 25:173–89.
[8] Yamada N, Okano T, Sakai H, Karikusa F, Sawasaki Y, Sakurai Y. Thermo-responsive polymeric surfaces; control of attachment and detachment of cultured cells. Die Makromolekulare Chemie, Rapid Commun 1990;11:571–6.
[9] Yamato M, Okanoa T. Cell sheet engineering. Mater Today 2004;7:42–7.
[10] L'Heureux N, Dusserre N, Konig G, Victor B, Keire P, Wight TN, et al. Human tissue-engineered blood vessels for adult arterial revascularization. Nat Med 2006;12:361–5.
[11] Yang J, Yamato M, Shimizu T, Sekine H, Ohashi K, Kanzaki M, et al. Reconstruction of functional tissues with cell sheet engineering. Biomaterials 2007; 28:5033–43.
[12] Wei F, Qu C, Song T, Ding G, Fan Z, Liu D, et al. Vitamin C treatment promotes mesenchymal stem cell sheet formation and tissue regeneration by elevating telomerase activity. J Cell Physiol 2012;227:3216–24.
[13] Bi Y, Ehirchiou D, Kilts TM, Inkson CA, Embree MC, Sonoyama W, et al. Identification of tendon stem/progenitor cells and the role of the extracellular matrix in their niche. Nat Med 2007;13:1219–27.
[14] Rui YF, Lui PPY, Li G, Fu SC, Lee YW, Chan KM. Isolation and characterization of multi-potent rat tendon-derived stem cells. Tissue Eng Part A 2010;16: 1549–58.
[15] Rui YF, Lui PP, Ni M, Chan LS, Lee YW, Chan KM. Mechanical loading increased BMP-2 expression which promoted osteogenic differentiation of tendon-derived stem cells. J Orthop Res 2011;29:390–6.
[16] Tan Q, Lui PP, Rui YF, Wong YM. Comparison of potentials of stem cells isolated from tendon and bone marrow for musculoskeletal tissue engineering. Tissue Eng Part A 2012;18:840–51.
[17] Ni M, Lui PP, Rui YF, Lee YW, Lee YW, Tan Q, et al. Tendon-derived stem cells (TDSCs) promote tendon repair in a rat patellar tendon window defect model. J Orthop Res 2012;30:613–9.
[18] Awad HA, Boivin GP, Dressler MR, Smith FN, Young RG, Butler DL. Repair of patellar tendon injuries using a cell-collagen composite. J Orthop Res 2003; 21:420–31.
[19] Harris MT, Butler DL, Boivin GP, Florer JB, Schantz EJ, Wenstrup RJ. Mesenchymal stem cells used for rabbit tendon repair can form ectopic bone and express alkaline phosphatase activity in constructs. J Orthop Res 2004;22: 998–1003.
[20] Wang JF, Olson ME, Ball DK, Brigstock DR, Hart DA. Recombinant connective tissue growth factor modulates porcine skin fibroblast gene expression. Wound Repair Regen 2003;11:220–9.
[21] Ivkovic S, Yoon BS, Popoff SN, Safadi FF, Libuda DE, Stephenson RC, et al. Connective tissue growth factor coordinates chondrogenesis and angiogenesis during skeletal development. Development 2003;130:2779–91.
[22] Chen CH, Cao Y, Wu YF, Bais AJ, Gao JS, Tang JB. Tendon healing in vivo: gene expression and production of multiple growth factors in early tendon healing period. J Hand Surg Am 2008;33:1834–42.
[23] Lee CH, Moioli EK, Mao JJ. Fibroblastic differentiation of human mesenchymal stem cells using connective tissue growth factor. Conf Proc IEEE Eng Med Biol Soc 2006;1:775–8.
[24] Lee CH, Shah B, Moioli EK, Mao JJ. CTGF directs fibroblast differentiation from human mesenchymal stem/stromal cells and defines connective tissue healing in a rodent injury model. J Clin Invest 2010;120:3340–9.
[25] Stone N, Meister A. Function of ascorbic acid in the conversion of proline to collagen hydroxyproline. Nature 1962;194:555–7.
[26] Nandi D, Patra RC, Swarup D. Effect of cysteine, methionine, ascorbic acid and thiamine on arsenic-induced oxidative stress and biochemical alterations in rats. Toxicology 2005;211:26–35.
[27] Korkmaz A, Kolankaya D. The protective effects of ascorbic acid against renal ischemia-reperfusion injury in male rats. Ren Fail 2009;31:36–43.
[28] Ji AR, Ku SY, Cho MS, Kim YY, Kim YJ, Oh SK, et al. Reactive oxygen species enhance differentiation of human embryonic stem cells into mesodermal lineage. Exp Mol Med 2010;42:175–86.
[29] Potdar PD, D'Souza SB. Ascorbic acid induces in vitro proliferation of human subcutaneous adipose tissue derived mesenchymal stem cells with upregulation of embryonic stem cell pluripotency markers Oct4 and SOX 2. Hum Cell 2010;23:152–5.
[30] Omeroğlu S, Peker T, Türközkan N, Omeroğlu H. High-dose vitamin C supplementation accelerates the Achilles tendon healing in healthy rats. Arch Orthop Trauma Surg 2009;129:281–6.
[31] Lui PPY, Cheuk YC, Hung LK, Fu SC, Chan KM. Increased apoptosis at late stage of tendon healing. Wound Repair Regen 2007;15:702–7.
[32] Lui PPY, Fu SC, Chan LS, Hung LK, Chan KM. Chondrocyte phenotype and ectopic ossification in collagenase-induced tendon degeneration. J Histochem Cytochem 2009;57:91–100.
[33] Langer R, Vacanti JP. Tissue engineering. Science 1993;260:920–6.
[34] Nishida K, Yamato M, Hayashida Y, Watanabe K, Yamamoto K, Adachi E, et al. Corneal reconstruction with tissueengineered cell sheets composed of autologous oral mucosal epithelium. N Engl J Med 2004;351:1187–96.
[35] Shimizu T, Sekine H, Yang J, Isoi Y, Yamato M, Kikuchi A, et al. Polysurgery of cell sheet grafts overcomes diffusion limits to produce thick, vascularized myocardial tissues. FASEB J 2006;20:708–10.
[36] Ohashi K, Yokoyama T, Yamato M, Kuge H, Kanehiro H, Tsutsumi M, et al. Engineering functional two- and three-dimensional liver systems in vivo using hepatic tissue sheets. Nat Med 2007;13:880–5.
[37] Ding G, Liu Y, Wang W, Wei F, Liu D, Fan Z, et al. Allogeneic periodontal ligament stem cell therapy for periodontitis. Stem Cells 2010;28: 1829–38.
[38] Jelinsky SA, Archambault J, Li L, Seeherman H. Tendon-selective genes identified from rat and human musculoskeletal tissues. J Orthop Res 2010;28: 289–97.
[39] Docheva D, Hunziker EB, Fassler R, Brandau O. Tenomodulin is necessary for tenocyte proliferation and tendon maturation. Mol Cell Biol 2005;25: 699–705.
[40] Schweitzer R, Chyung JH, Murtaugh LC, Brent AE, Rosen V, Olson EN, et al. Analysis of the tendon cell fate using Scleraxis, a specific marker for tendons and ligaments. Development 2001;128:3855–66.
[41] Murchison ND, Price BA, Conner DA, Keene DR, Olson EN, Tabin CJ, et al. Regulation of tendon differentiation by scleraxis distinguishes force-transmitting tendons from muscle-anchoring tendons. Development 2007; 134:2697–708.
[42] Wang B, Liu W, Zhang Y, Jiang Y, Zhang WJ, Zhou G, et al. Engineering of extensor tendon complex by an ex vivo approach. Biomaterials 2008;29: 2954–61.
[43] Cao D, Liu W, Wei X, Xu F, Cui L, Cao Y. In vitro tendon engineering with avian tenocytes and polyglycolic acids: a preliminary report. Tissue Eng 2006;12: 1369–77.
[44] Saber S, Zhang AY, Ki SH, Lindsey DP, Smith RL, Riboh J, et al. Flexor tendon tissue engineering: bioreactor cyclic strain increases construct strength. Tissue Eng Part A 2010;16:2085–90.
[45] Abousleiman RI, Reyes Y, McFetridge P, Sikavitsas V. Tendon tissue engineering using cell-seeded umbilical veins cultured in a mechanical stimulator. Tissue Eng Part A 2009;15:787–95.

[46] Ouyang HW, Goh JC, Thambyah A, Teoh SH, Lee EH. Knitted poly-lactide-co-glycolide scaffold loaded with bone marrow stromal cells in repair and regeneration of rabbit Achilles tendon. Tissue Eng 2003;9:431–9.
[47] Kryger GS, Chong AK, Costa M, Pham H, Bates SJ, Chang J. A comparison of tenocytes and mesenchymal stem cells for use in flexor tendon tissue engineering. J Hand Surg Am 2007;32:597–605.
[48] Juncosa-Melvin N, Boivin GP, Gooch C, Galloway MT, West JR, Dunn MG, et al. The effect of autologous mesenchymal stem cells on the biomechanics and histology of gel-collagen sponge constructs used for rabbit patellar tendon repair. Tissue Eng 2006;12:369–79.
[49] Chong AK, Ang AD, Goh JC, Hui JH, Lim AY, Lee EH, et al. Bone marrow-derived mesenchymal stem cells influence early tendon-healing in a rabbit Achilles tendon model. J Bone Jt Surg Am 2007;89:74–81.
[50] Hankemeier S, van Griensven M, Ezechieli M, Barkhausen T, Austin M, Jagodzinski M, et al. Tissue engineering of tendons and ligaments by human bone marrow stromal cells in a liquid fibrin matrix in immunodeficient rats: results of a histologic study. Arch Orthop Trauma Surg 2007;127:815–21.